Journal of Power Sources 245 (2014) 745–751

Contents lists available at SciVerse ScienceDirect

Journal of Power Sources

journal homepage: www.elsevier.com/locate/jpowsour

Stress evolution and capacity fade in constrained lithium-ion pouch cells

John Cannarella, Craig B. Arnold*,[1]

Department of Mechanical and Aerospace Engineering, Princeton University, Princeton, NJ 08544, USA

HIGHLIGHTS

- Stack stress is a dynamic quantity that evolves during electrochemical cycling.
- The initial applied stack pressure determines how stress evolves during cycling.
- Small stack stresses prevent layer delamination, benefiting long term performance.
- Higher stress causes higher rates of capacity fade through cycleable lithium loss.
- Stack stress leads to localized separator deformation and chemical degradation.

ARTICLE INFO

Article history:
Received 4 June 2013
Received in revised form
28 June 2013
Accepted 30 June 2013
Available online 13 July 2013

Keywords:
Lithium-ion battery
Mechanical stress
Capacity fade
Cell aging
Surface film
Cycle life

ABSTRACT

The effects of mechanical stress on lithium-ion battery life are investigated by monitoring the stack pressure and capacity of constrained commercial lithium-ion pouch cells during cycling. Stack stress is found to be a dynamic quantity, fluctuating with charge/discharge and gradually increasing irreversibly over long times with cycling. Variations in initial stack pressure, an important controllable manufacturing parameter, are shown to produce different stress evolution characteristics over the lifetime of the cells. Cells manufactured with higher levels of stack pressure are found to exhibit shorter cycle lives, although small amounts of stack pressure lead to increased capacity retention over unconstrained cells. Postmortem analysis of these cells suggests a coupling between mechanics and electrochemistry in which higher levels of mechanical stress lead to higher rates of chemical degradation, while layer delamination is responsible for the capacity fade in unconstrained cells. Localized separator deformation resulting in nonuniform lithium transport is also observed in all cells.

1. Introduction

Lithium-ion batteries are finding application in many large scale technologies such as electric vehicles, aerospace, and grid level storage. For such applications it is necessary to develop batteries with long cycle and calendar lives as battery replacement is impractically expensive. To this end there have been many studies investigating the various competing aging mechanisms that occur in lithium-ion batteries such as SEI growth, electrode material loss, and separator pore closure [1–3]. These aging studies consider a wide range of parameters (e.g. state of charge, depth of discharge, charge/discharge rate, charge variability, and temperature) to better understand the effects of different operating/environmental conditions on aging [4,5]. One important parameter that has been neglected in the literature is the effect of compressive stack pressure on lithium-ion battery aging.

Compressive stack pressure is present in all lithium-ion batteries and is used to maintain intimate contact between battery components as well as to prevent layer delamination and deformation during operation. This stack pressure is applied during manufacturing when the electrode stack is placed into a rigid constraint and is typically in the range of 0.1–1 MPa. Examples of rigid constraints are the rigid housings placed over pouch cells in design applications or the canisters of cylinder or prismatic cells. While the initial application of this stack stress is controlled during battery manufacturing, this stress is a dynamic quantity that varies over the lifetime of the cell. During operation the compressive stress at the stack level within the cell fluctuates owing to expansion of the electrodes within a constrained environment. The issue

* Corresponding author.
E-mail address: cbarnold@princeton.edu (C.B. Arnold).
[1] URL: princeton.edu/~spikelab.

0378-7753/$ – see front matter © 2013 Elsevier B.V. All rights reserved.
http://dx.doi.org/10.1016/j.jpowsour.2013.06.165

of mechanical stress becomes increasingly important as higher capacity materials with higher volumetric expansions (e.g. silicon) are incorporated into battery electrodes. Other competing mechanisms such as SEI growth [6], binder swelling [7], and viscoelastic creep [2] further complicate prediction of stack level stress evolution in batteries.

Typical studies on mechanical stress evolution in lithium-ion cells focus on stress arising within individual electrode particles or within the plane of the composite electrodes [7–9]. These particle level and composite electrode level stresses have been linked to capacity fade through particle exfoliation and SEI growth mechanisms. Previous work has also suggested links between stack level mechanical stress and capacity fade [2,3], but no publications have explicitly investigated stack level stress in lithium-ion cells and its effects on capacity fade. To date there has been only a limited number of studies on the subject of stack level stress: a few experimental measurements of stack level stress evolution [10,11] and thickness changes [12] during cycling, as well as well as numerical simulations of stress induced in the separator by electrode expansion [13].

This paper focuses on measuring the stack level stress evolution in constrained commercial pouch cells and its effect on rate of capacity fade. It is shown that the level of initial stack pressure can strongly influence the stress evolution and capacity fade characteristics of cells, with higher stress levels showing higher rates of capacity fade. A postmortem analysis of the cycled cells indicates that loss of cycleable lithium is the main failure mechanism, with higher stressed cells exhibiting higher rates of capacity fade. These results suggest an important coupling between mechanical stress and chemical degradation, possibly through inhomogeneous electrode utilization due to transport restriction from separator deformation [3].

2. Experimental

Commercial 500 mAh pouch cells with nominal dimensions of 25 mm × 35 mm × 6.5 mm are used in this study. The active materials are lithium cobalt oxide and graphite and the electrolyte is $LiPF_6$ in organic solvent. These cells are initially discharged at a C/2 rate until reaching a 2.7 V cutoff before being placed into the constraint fixture shown schematically in Fig. 1. Subsequent charging results in stress build up due to electrode expansion.

The constraint fixture consists of a pouch cell in series with an amplified load cell. An aluminum plate is placed between the pouch cell and load cell to distribute the mechanical load evenly along the flat face of the pouch cell. The load cell and pouch cell assembly is then clamped down between two aluminum plates held together with nuts and bolts. Prior to tightening the nuts, a controlled load is applied with a compression testing machine according to the initial load prescribed in Table 1. After the initial load is applied the nuts

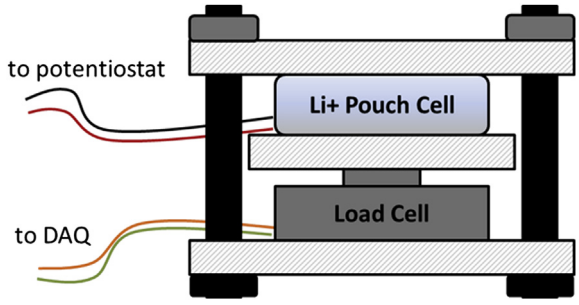

Fig. 1. Schematic of the constraint fixture used to maintain and measure compressive stack stress.

Table 1
Summary of cell stack pressures in MPa. Initial is the stack pressure applied before stress relaxation occurs. Min and Max correspond to the minimum and maximum stresses experienced by the cells after stress relaxation.

Stack pressure	Initial	Min	Max
Unconstrained	–	–	–
Low	0.05	0	0.5
Medium	0.5	0.2	1.5
High	5	1	3

are gently secured in position and thread-locking adhesive is applied to prevent the nuts from loosening during the cycling portion of the test. The constraint fixture with pouch cell is removed from the compression tester for electrochemical cycling.

The pouch cells are cycled using a C/2 CCCV scheme between 4.2 V and 2.7 V with a C/50 cutoff. The cells are cycled at room temperature, although precise temperature control is not used. Mechanical and electrical data is collected every 10 min. After cycling, the pouch cells are disassembled in an argon atmosphere containing less than 0.1 ppm water vapor and oxygen. Coin cells are fabricated using electrodes harvested from the pouch cells. These electrodes have the active material removed from one side to expose the current collector for good electrical connection. The area of the negative electrode in each cell is slightly larger than the area of the positive electrode to prevent misalignment. The graphite anodes half cells are cycled between 0.01 V and 1.3 V, and the lithium cobalt oxide half cells are cycled between 2.8 and 4.3 versus lithium.

3. Results and discussion

3.1. Mechanical stress evolution

Typical plots of compressive stack stress as a function of time for cells held at different stack pressures are shown in Fig. 2 for early times and in Fig. 3 for the entire duration of the cycling test. To understand these stress evolution plots of the constrained pouch cells it is necessary to first understand the constant thickness nature of the rigid constraint. The constraint shown in Fig. 1 constrains the pouch cell to maintain a constant thickness such that stress, not thickness, is free to evolve. Stress changes therefore correspond to the cell thickness changes that would occur in the

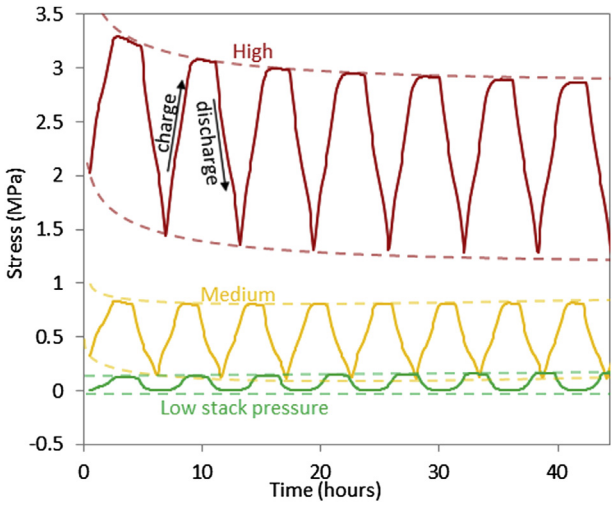

Fig. 2. Stack stress evolution at early times. The high and medium stack pressure cells exhibit stress relaxation spanning time scales on the order of days.

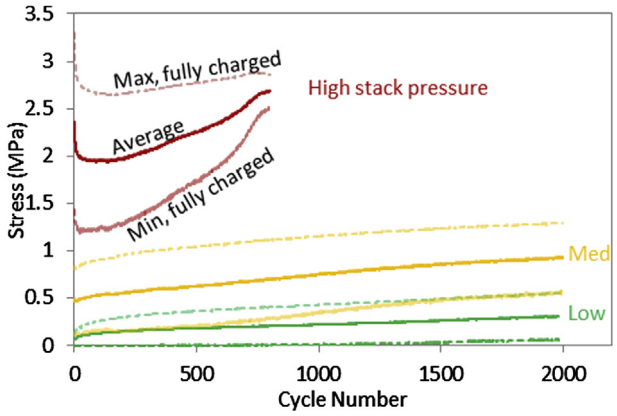

Fig. 3. Stack stress evolution as a function of cycle number. Changes in the initial stack pressure have a profound effect on the nature of the subsequent stress evolution in the cell.

absence of a rigid constraint, with the measured stress change being equal to the applied stress necessary to reverse the cell thickness change. The constant thickness scenario provides a good description of commercial batteries which are generally placed in rigid constraints.

A consequence of the constant thickness loading scheme used in batteries and the viscoelastic nature of battery materials is that stress relaxation will occur, especially at early time scales. Conceptually, stress relaxation can be understood by considering the simple Maxwell model of viscoelasticity which contains a spring element (purely elastic with modulus E) and dashpot element (purely viscous with viscosity η) in series. When an instantaneous deformation is applied to the Maxwell system there occurs an initial stress σ_0 which relaxes with time t according to the well known expression [14]

$$\sigma(t) = \sigma_0 \exp -\frac{E}{\eta} t$$

Taking the derivative shows that the rate of stress relaxation is dependent on stress level so that pouch cells held at higher stress levels should exhibit higher degrees of stress relaxation:

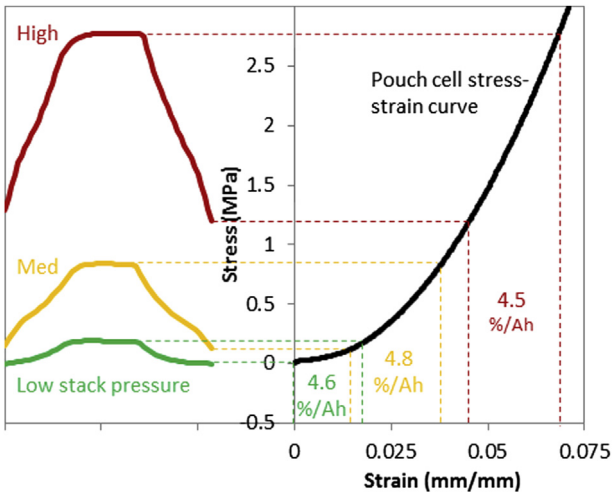

Fig. 4. Stress–time curves from Fig. 2 plotted with a pouch cell stress–strain curve showing that the different magnitude stress fluctuations correspond to the same levels of cell expansion normalized by charge.

$$\frac{d\sigma(t)}{dt} = -\frac{E}{\eta}\sigma(t)$$

This conceptual treatment has a couple of implications. First, the initial applied stack stress is only felt by the battery stack for an instant before relaxing to some other equilibrium value which depends on the material properties, rate of loading, and initial stress. This is the reason that the initial discharged stresses shown in Fig. 2 are much lower than the prescribed initial stack pressures in Table 1: by the time the load cells are attached to the DAQ, the stack stress has relaxed significantly. The ephemeral nature of the initial applied stress makes initial stress a somewhat arbitrary designation of stack pressure. Better descriptions of stack pressure can be given by minimum, maximum and/or average stress values. The second implication is that the higher stressed cells should exhibit higher degrees of stress relaxation, which is evident from Fig. 3 with the high stack pressure cells showing stress relaxation on a time scale of days, the medium stack pressure cells showing relaxation on a time scale of hours, and the low stack pressure cells showing relaxation on a time scale of seconds.

The next notable feature of the stress evolution data is that stress state varies with charge state. This is due to expansion of both the graphite and lithium cobalt oxide electrodes with charging [15]. Even though the thickness of the pouch cell as a whole is held constant by the rigid constraint, the electrodes are still able to expand into the separator, which acts like a spring by building up stress as it is compressed – this is the source of the stress fluctuations on charging. The stress compresses the electrodes to a lesser extent than the separator because the electrodes are much more rigid than the separator. Detailed analysis of single-cycle curves of stack stress evolution in constrained cells and thickness evolution in unconstrained cells can be found in Refs. [10–12,16].

While cells under each of the different stack pressures exhibit state of charge dependent stress fluctuations, the magnitudes of the stress fluctuations are observed to be larger in the more highly stressed cells. This observation can be explained by considering the nonlinear elastic mechanical properties of the pouch cell. If the pouch cell were linear elastic, the electrode expansion with charging would be expected to produce the same magnitude of stress fluctuation regardless of stress level. However, from the pouch cell's stress–strain curve shown in Fig. 4, it can be seen that the pouch cell is more rigid at higher stress levels. This means that for the same amount of electrode expansion, cells with higher stack pressures will exhibit higher charging stress fluctuations.

One feature that is not apparent in the early time scale stress evolution plot is the trend of gradual stress increase that occurs in constrained lithium-ion cells. This gradual stress accumulation occurs on time scales much larger than stress relaxation and charging stresses, and is indicative of a gradual overall volumetric expansion of the cell. Possible explanations for the persistent stress increase are cycling-induced structural changes within the electrode particles [17,18] and growth of the SEI [6], which result in a permanent volumetric expansion that creates additional mechanical stress. Upon disassembly, the graphite anodes taken from all of the cycled cells are indeed found to be thicker than pristine anodes, consistent with the stress increases seen in Fig. 3 and observations made in previous studies [19]. The implication of this stress increase is that the stress in a lithium-ion cell during its service life is likely to be much higher than the initial manufacturing stack pressure.

3.2. Electrochemical characterization

The ultimate result of the accumulation of mechanical stress in the constrained pouch cells is a reduction in electrochemical performance, with higher stress levels leading to higher rates of capacity fade. This effect is readily seen in Fig. 5 which shows capacity

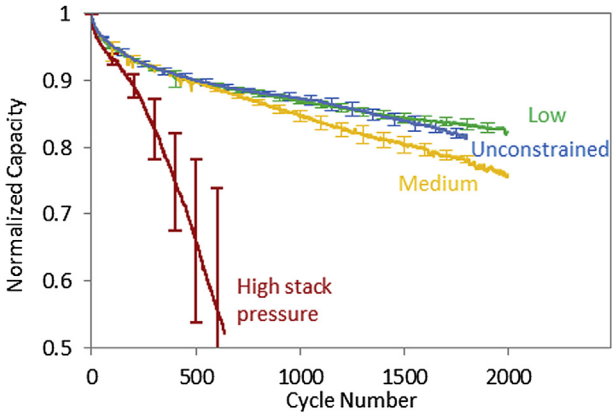

Fig. 5. C/2 capacity averaged overall three cells at each stack pressure as a function of cycle number. Error bars show +/− one standard deviation.

as a function of cycle number. Note that plotting capacity against time instead of cycle number produces essentially the same plot. Fig. 5 shows an important exception to the general trend of higher levels of stress leading to higher rates of capacity fade, with the unconstrained cells exhibiting a higher rate of capacity fade than the low stack pressure cells after about 1000 cycles. The higher capacity retention exhibited by the low stack pressure cells over the unconstrained cells shows that a small amount of compression is indeed beneficial for long term cell performance. In all of the cells except the high stack pressure cells, there is no substantial reversal in capacity loss upon slower cycling.

To better understand the effects of stress on the capacity fade behavior of the cycled cells, a postmortem analysis is conducted in which the cycled pouch cells are disassembled under inert atmosphere and the individual cell components are analyzed. Striking macroscopic visual differences are observed between cells held at different stack pressures as shown in Fig. 6, especially with respect to a pristine pouch cell. Note that the disassembled cells are at different charge states as indicated in the figure, which is the source of the difference in color (yellow vs. black) between the pictured anodes. One clear visual trend is that there exists a solid surface film on the anodes taken from the constrained cells, with the cells constrained at a higher stack pressure showing larger regions of film coverage. The film can be seen on the anodes and to a lesser extent on the separator face that was in contact with the anodes. The silver-colored portions of the cathodes are regions where the cathode material adhered to the separator and delaminated from the cathode during disassembly, not regions covered with a surface film. These observations are consistent among all the cells in the study and suggest a coupling between mechanics and chemical degradation.

The notion of a coupling between mechanics and chemistry is further corroborated by the fact that the anode surface films appear in a periodic pattern along the face of the electrode such that when the electrodes are rolled back into a jelly roll the regions of film coverage are all aligned. This alignment is indicative of mechanical effects because vertically aligned regions would experience similar localized mechanical environments, but not necessarily similar localized chemical environments. This also suggests that the mechanical stress within the constrained pouch cells is not uniform. Despite the apparent importance of local environment, no clear preference for formation on either the flat faces or rounded edges is observed when comparing all of the disassembled cells from this study (including cells not pictured in Fig. 6). At present, the chemical composition and formation mechanism of the anode surface films are unknown. However, because the stack pressures in the constrained pouch cells are relatively low from a thermodynamic perspective, it is likely that these films form through a kinetic effect, possibly due to nonuniform current distributions caused by the localized regions of high deformation within the stressed separator observed in Fig. 7. Full characterization is beyond the scope of this work and will be the subject of a subsequent study.

The assertion of a nonuniform current distribution is supported by the photograph of the medium stack-pressure cell in Fig. 6. This cell is partially charged before disassembly to allow visual

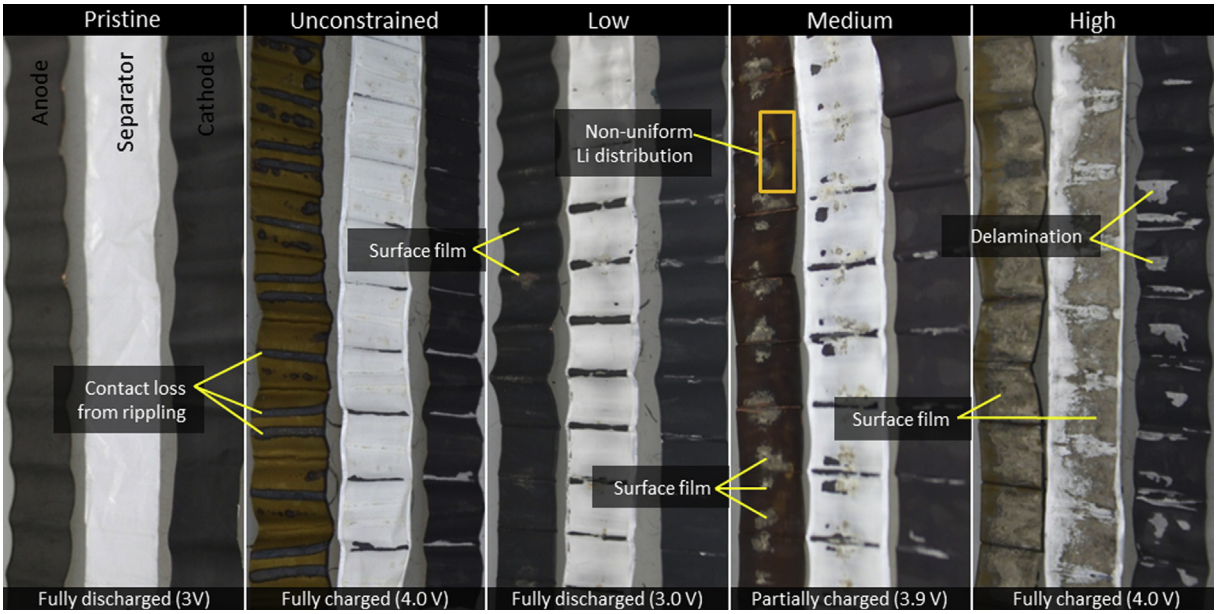

Fig. 6. Photographs of the disassembled pouch cells showing different types of mechanical stress dependent degradation. The boxed portion underscores an area where the spatially nonuniform lithium distribution within the anode is particularly visible, with black, red, and yellow colored regions in close proximity. Similar lithium distributions can be seen on each face of the partially charged medium stack pressure anode. (For interpretation of the references to color in this figure legend, the reader is referred to the web version of this article.)

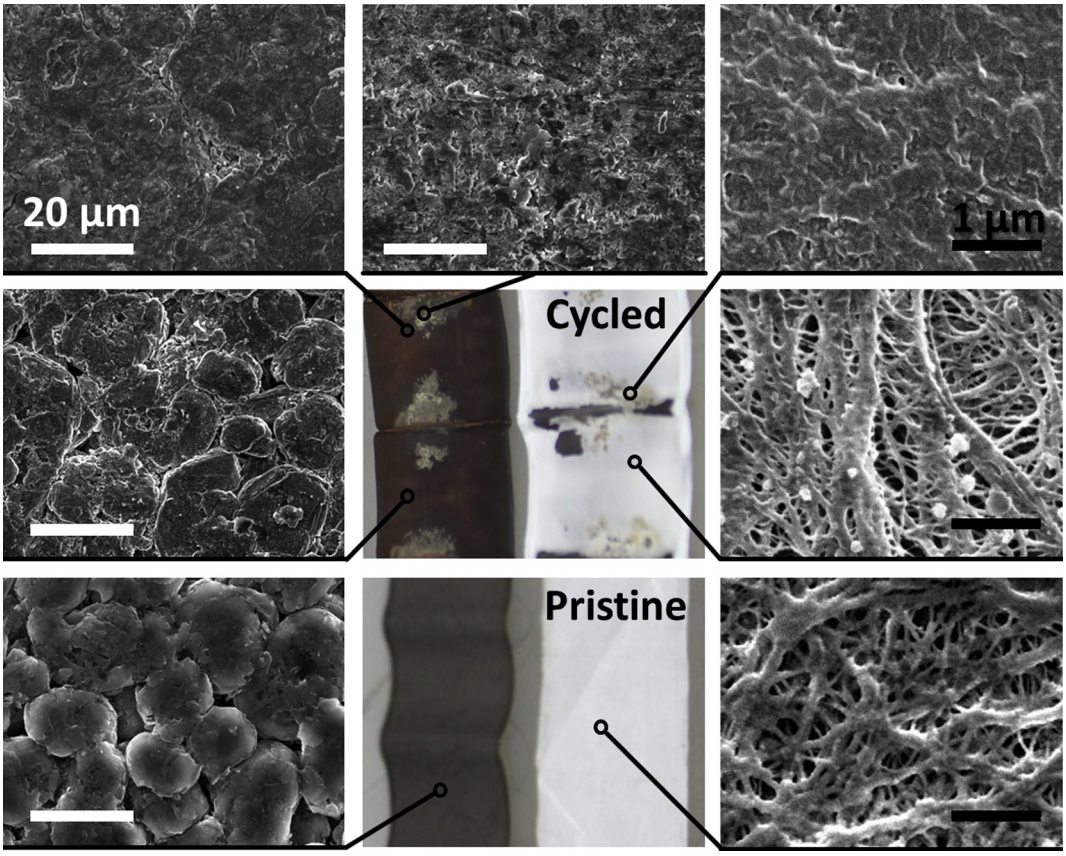

Fig. 7. SEM micrographs of separators and anodes from pristine and a cell cycled at medium stack pressure showing spatially nonuniform degradation.

inspection of the lithium distribution, since graphite changes from black to red to gold in color with increasing lithium concentration [20]. As can be seen in the boxed portion of Fig. 6, the partially charged anode contains regions of black, red, and gold color in close proximity to each other, indicating a highly nonuniform spatial distribution of intercalated lithium within the electrodes. Nonuniform lithium distributions similar to the boxed region can be seen occurring on each face along the entire length of the medium stack pressure anode. While the nonuniform anode coloration could conceivably be caused by local electronic disconnection of graphite particles [1], in this case nonuniform lithium transport through the separator is a more likely explanation since the anodes retain near full capacity after cycling, as shown later in Fig. 8.

Visual inspection of the disassembled pouch cells also reveals an important difference between the mechanical behavior during cycling of the unconstrained and constrained pouch cells. In the unconstrained pouch cell, the originally flat faces of the wound electrodes exhibit a rippled structure after cycling such that certain regions of the flat faces have lost contact with the separator. Electrode rippling is a consequence of cycling (not to be confused with the rounded edges formed from the winding of the electrode stack) and has been reported previously in a study investigating anode expansion in pouch cells [21]. This rippling results in contact loss with the separator, disconnecting these regions from the rest of the cell such that they no longer contribute to the cell's capacity.

The local disconnection resulting from rippling is readily visualized when the unconstrained pouch cells are fully charged before disassembly such that the lithiated graphite shows a yellow color and unlithiated graphite remains black. In Fig. 6 the black regions of the unconstrained anode correspond to regions of the anode that have loss contact with the separator as a result of rippling. Like the solid films observed in the constrained cells, these disconnected regions are periodic along the face of the electrode such that they are vertically aligned when the electrodes are rolled into a stack, highlighting the mechanical nature of this effect. One can also see slight differences in color of the unconstrained separator that resulted from the rippling during operation. This loss of electrode contact due to rippling is likely responsible for the lower capacity retention of the unconstrained cells compared with the lightly constrained cells. Thus a small amount of mechanical compression

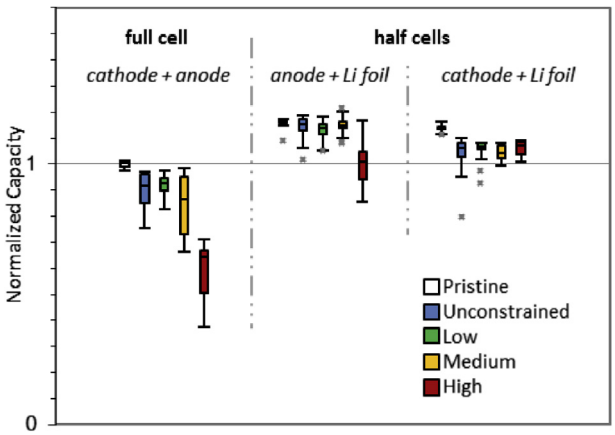

Fig. 8. Five number summaries (minimum, lower quartile, median, upper quartile, maximum) of the capacity data for post-mortem coin cells assembled with cycled electrodes. "Control" cells contain pristine electrodes instead of cycled electrodes. Individual data points are outliers falling outside 1.5 times the interquartile range.

is beneficial to long term performance by preventing layer delamination through rippling.

There are also clear microscopic visual differences between the cycled cells and pristine cells when viewed under SEM. Fig. 7 shows SEM images of the anodes and separators of a pristine cell and a cycled cell. Prior to imaging, the separators are rinsed multiple times in DMC to remove any material loosely adhered to the surface to allow visualization of the pore structure. The electrodes are left unrinsed so as to minimize disturbance to any surface features. SEM images of the cathodes are not included in Fig. 7 as there are no clear visual differences between any of the cathodes. The samples are carried to the SEM under argon atmosphere and are only exposed to ambient atmosphere between transferring from a sealed vessel to the SEM vacuum chamber. Exposure to atmosphere is minimized because it is observed that some of the visible surface features tend to disappear over time in ambient atmosphere.

Fig. 7 shows an anode from a cell cycled under medium stack pressure with SEM images taken at different positions along the anode. When viewed under SEM one can see that the surface film on the anode extends beyond the portion of the film visible to the naked eye, as shown in the central image of Fig. 7. Fig. 7 also shows the spatially heterogeneous nature of these films, with a portion of the anode being free from film coverage. Similar features can be seen in the low and high stack pressure cells, though as might be expected from Fig. 6, the amount of film coverage increases with stack pressure. In the high stack pressure cells, the anode is found to be completely covered with a surface film during SEM imaging, with the exception of a narrow region around the edge of the anode. This edge region remains inactive during cycling because it is not directly opposite the cathode (the anode is slightly larger than the cathode in the pouch cell), suggesting that the film formation is heavily influenced by cycling behavior, not just time.

The SEM images of the separators from all of the cycled cells show reductions in porosity when compared to a separator taken from a pristine cell as shown in Fig. 7. With the exception of the high stack pressure cells, pore closure is found to be spatially heterogeneous, occurring in localized regions that are periodic along the length of the separator. The surface morphology of the reduced-porosity regions looks similar to the surface morphology of pristine separators that have been mechanically deformed at high stresses for short times [2]. The deformed morphology is indicative of mechanical creep which has occurred at stresses below the yield point of the polyethylene separator material, even in the unconstrained cell. Thus in the absence of an external mechanical constraint, some stress must still build up as the layers expand under the constraint imposed by the jelly rolled composite electrode structure.

It is important to note that the separators in Fig. 7 are not held under mechanical stress during imaging. If it were possible to obtain SEM images of separators under the mechanical compression characteristic of operation in a real cell, one would see an even higher degree of pore reduction owing to elastic deformation of the separator material [3]. Such closure of pores directly leads to uneven lithium transport and distribution, which is evidenced by nonuniform color distributions in pristine anodes lithiated in coin cells with cycled separators. It is possible that such heterogeneous operation facilitates the increased chemical degradation observed in the constrained pouch cells.

To shed light on the dominant source of the capacity fade observed in Fig. 5, a capacity analysis of coin cells assembled with electrodes harvested from the cycled pouch cells is conducted. The postmortem capacity measurements are presented in Fig. 8 using a five number summary to show the variability of the capacity measurements. Both half cells and full cells assembled with cycled electrodes show higher variability in measured capacity than the control cells assembled with pristine electrodes. The higher capacity variability of the full cells assembled with cycled electrodes is likely a result of the nonuniform spatial distribution of intercalated lithium that is observed within the electrodes: a full cell assembled with a pair of electrodes containing an above or below average amount of intercalated lithium results in an above or below average measured capacity, respectively. The higher variability of the cycled electrode half cells suggests that some degree of spatially heterogeneous electrode degradation has occurred. The electrode degradation appears independent of stress with the exception of the anodes harvested from the high stack pressure cells.

The capacity analysis indicates that the source of capacity fade in all of the constrained pouch cells is loss of cycleable lithium. This conclusion follows from Fig. 8, which shows that the half cells have higher capacities than their corresponding full cells. This means that the capacity of the full cell is limited not by either individual electrode, but rather by the amount of cycleable lithium available to the cell for intercalation. Thus the capacity for each pouch cell under study is determined directly by its cycleable lithium content and the capacity fade is a measure of irreversible lithium consumption by side reactions. The trend of increasing loss of cycleable lithium with increasing stack stress further supports the notion of a coupling between mechanics and chemical degradation. Presumably, much of this lost lithium is contained within the visible solid surface films formed on the anodes shown in Fig. 6, but chemical analysis of these films is out of scope of the current work.

4. Conclusion

Stack level mechanical stress is a dynamic quantity that evolves in constrained lithium ion cells through the competing effects of viscoelastic stress relaxation, lithiation-induced expansion/contraction during charge/discharge, and gradual permanent increases in electrode volume. All cells in this study exhibit persistent long-term increases in stress indicating that in practice stack stresses may be much higher than the initially applied stack pressure. Stack level stress is shown to have a strong effect on long term cell performance, with higher levels of stress leading to higher rates of capacity fade in the cells under study. Upon disassembly, localized deformation in the separator and surface film coverage on the anode are observed in all cells. Film coverage is found to increase with mechanical stress, suggesting a coupling between mechanical stress and chemical degradation. The observed capacity fade in all cells is attributed to loss of cycleable lithium through a postmortem analysis, corroborating the notion of mechanically mediated chemical degradation. Light stack pressure is found to be beneficial to long term performance by preventing layer delamination.

Acknowledgments

J.C. acknowledges the Department of Defense (DoD) for support through the National Defense Science and Engineering Graduate Fellowship (NDSEG) Program. We also acknowledge support from the Princeton University Siebel Energy Grand Challenge, the Princeton University Carbon Mitigation Initiative, and the Rutgers-Princeton NSF IGERT in Nanotechnology for Clean Energy. We acknowledge the usage of the PRISM Imaging and Analysis Center, which is supported in part by NSF-MRSEC.

References

[1] J. Vetter, P. Novák, M. Wagner, C. Veit, K.-C. Möller, J. Besenhard, M. Winter, M. Wohlfahrt-Mehrens, C. Vogler, A. Hammouche, Journal of Power Sources 147 (2005) 269–281.
[2] C. Peabody, C.B. Arnold, Journal of Power Sources 196 (2011) 8147–8153.
[3] J. Cannarella, C. Arnold, Journal of Power Sources 226 (2013) 149–155.

[4] J. Wang, P. Liu, J. Hicks-Garner, E. Sherman, S. Soukiazian, M. Verbrugge, H. Tataria, J. Musser, P. Finamore, Journal of Power Sources 196 (2011) 3942–3948.
[5] Z. Li, L. Lu, M. Ouyang, Y. Xiao, Journal of Power Sources 196 (2011) 9757–9766.
[6] A. Mukhopadhyay, A. Tokranov, X. Xiao, B.W. Sheldon, Electrochimica Acta 66 (2012) 28–37.
[7] V. Sethuraman, M. Chon, M. Shimshak, V. Srinivasan, P. Guduru, Journal of Power Sources 195 (2010) 5062–5066. Cited by (since 1996) 56.
[8] M.J. Chon, V.A. Sethuraman, A. McCormick, V. Srinivasan, P.R. Guduru, Physical Review Letters 107 (2011) 045503.
[9] Y.-T. Cheng, M.W. Verbrugge, Journal of Power Sources 190 (2009) 453–460.
[10] X. Wang, Y. Sone, G. Segami, H. Naito, C. Yamada, K. Kibe, Journal of The Electrochemical Society 154 (2007) A14.
[11] X. Wang, Y. Sone, S. Kuwajima, Journal of The Electrochemical Society 151 (2004) A273.
[12] J.H. Lee, H.M. Lee, S. Ahn, Journal of Power Sources 119–121 (2003) 833–837.
[13] D. Shi, X. Xiao, X. Huang, H. Kia, Journal of Power Sources 196 (2011) 8129–8139.
[14] Mechanical Properties of Engineered Materials, Marcel Dekker, Inc.
[15] Y. Koyama, T. Chin, U. Rhyner, R. Holman, S. Hall, Y.-M. Chiang, Advanced Functional Materials 16 (2006) 492–498.
[16] T.E. Chin, U. Rhyner, Y. Koyama, S.R. Hall, Y.-M. Chiang, Electrochemical and Solid-State Letters 9 (2006) A134.
[17] D. Liu, Y. Wang, Y. Xie, L. He, J. Chen, K. Wu, R. Xu, Y. Gao, Journal of Power Sources 232 (2013) 29–33.
[18] V.A. Sethuraman, L.J. Hardwick, V. Srinivasan, R. Kostecki, Journal of Power Sources 195 (2010) 3655–3660.
[19] R.S. Rubino, H. Gan, E.S. Takeuchi, Journal of The Electrochemical Society 148 (2001) A1029.
[20] Y. Qi, S.J. Harris, Journal of The Electrochemical Society 157 (2010) A741.
[21] N. Zhang, H. Tang, Journal of Power Sources 218 (2012) 52–55.